RSC Sustainability

ROYAL SOCIETY OF CHEMISTRY

PAPER

View Article Online
View Journal | View Issue



Cite this: *RSC Sustainability*, 2024, **2**, 491

# Synthesis of fine Na-type zeolite grains from coal fly ash and the assessment of the adsorption capability of lead ions from aqueous solutions

Fumihiko Ogata,[a] Noriaki Nagai,[a] Yugo Uematsu,[a] Yuhei Kobayashi,[a] Nanako Kitamura,[a] Chalermpong Saenjum[bc] and Naohito Kawasaki *[ad]

Received 11th November 2023
Accepted 19th December 2023

DOI: 10.1039/d3su00421j

rsc.li/rscsus

Fine Na-type zeolite grains (ZE) were prepared by dry milling treatment (D-ZE) or wet milling treatment (W-ZE). Then, the prepared samples were characterized. The effective parameters of adsorption capacities including the initial concentration, adsorption temperature, pH, and contact time for lead-ion adsorption were determined. The results revealed that the adsorption capacity of lead ions was in the order of ZE (32.7 mg $g^{-1}$) < D-ZE (70.7 mg $g^{-1}$) < W-ZE (166.9 mg $g^{-1}$). The results of the adsorption processes exhibited increased adsorption temperature, an increased pH of up to 5.0, and increased contact time. Pseudo-second-order model kinetic was observed, and the lead adsorbent isotherm followed the Langmuir and Freundlich models. Finally, one of the adsorption mechanisms was elucidated by analyzing the binding energy of lead (Pb) and lead (Pb) distribution before and after adsorption. Thus, the results serve as useful information for the adsorption of lead ions from aqueous solutions using ZE samples.

**Sustainability spotlight**

Recently, the "Ensure Availability and Sustainable Management of Water and Sanitation for All" goal (Goal 6) was adopted by all United Nations members as one of the goals of Sustainable Development Goals. In this study, we focused on coal fly ash that can be recycled (only by ~25%) as a raw material for cement production. Therefore, it is necessary to evaluate the recycling technologies using coal fly ash for waste reduction and/or for preparing value-added materials. This study aimed to explore the potential utilization of coal fly ash as a raw material to synthesize zeolites (adsorbent). Moreover, the capacity of the synthesized fine zeolite grains to adsorb lead ions and their adsorption mechanism are demonstrated.

## 1. Introduction

Ensuring water quality is important for humans as well as for all other living things.[1] Recently, the "Ensure Availability and Sustainable Management of Water and Sanitation for All" goal (Goal 6) was adopted by all United Nations members as one of the goals of Sustainable Development Goals. The members are aggressively working toward achieving this goal. In this regard, the pollution of water supply is a serious concern worldwide.[2]

The contamination of environmental water by heavy metals is one of the important problems. According to the World Health Organization, lead (Pb) is currently one of the most toxic metals in environmental water.[3] In addition, the Agency for Toxic Substances and Disease Registry and the International Agency for Research on Cancer have also regarded lead to have high toxicity among all substances.[4,5] In an aquatic ecosystem, lead (Pb(II)) ions are harmful due to their nonbiodegradability and latent accumulation in the ecosystem that potentially cause serious health problems.[6] These lead ions are released into the water environment from various industries, including plating, agriculture, pigment, tanning, battery, and oil refining.[7]

The maximum residue limit (MRL) of lead concentrations in drinking and wastewater is 0.005 and 0.05 mg $L^{-1}$, respectively.[8] Various physicochemical techniques, including chemical precipitation, electrochemical reduction, ion exchange, membrane separation, reverse osmosis, and adsorption, have been employed to remove lead ions from the water environment.[9] Adsorption treatment using an adsorbent is a widely used process for removing heavy metals, such as lead ions, from aqueous media owing to its low cost, easy operation, the possibility of use in batches, continuity, application at low concentrations, and regeneration or reuse of adsorbed metals.[10,11]

On the other hand, it is desirable to increase coal-fire power generation by up to 46% of the total electricity production by

[a]*Faculty of Pharmacy, Kindai University, 3-4-1 Kowakae, Higashi-Osaka, Osaka 577-8502, Japan. E-mail: kawasaki@phar.kindai.ac.jp*

[b]*Faculty of Pharmacy, Chiang Mai University, Suthep Road, Muang District, Chiang Mai 50200, Thailand*

[c]*Center of Excellence for Innovation in Analytical Science and Technology for Biodiversity-based Economic and Society (I-ANALY-S-T_B.BES-CMU), Chiang Mai University, Chiang Mai 50200, Thailand*

[d]*Antiaging Center, Kindai University, 3-4-1 Kowakae, Higashi-Osaka, Osaka 577-8502, Japan*

2030.[12] Accordingly, approximately 800–900 million tons per year of coal fly ash, a by-product from the combustion of coal, is generated worldwide. In this study, we focused on coal fly ash that can be recycled (only by ~25%) as a raw material for cement production and can replace clay components, soil conditioners, and fertilizers.[13–17] However, a major portion has been disposed of in landfills. Therefore, it is necessary to evaluate the recycling technologies using coal fly ash for waste reduction and/or for preparing value-added materials.

Hydrothermal activation treatment[18] can be used to recycle coal fly ash into zeolites and adsorbents. Zeolite materials are an ideal adsorbent for removing heavy metals from wastewater due to their high cation exchange capacity, thermal stability, and excellent affinity to heavy metals.[19,20] Additionally, many researchers have successfully demonstrated the effective removal of heavy metals from aqueous media using zeolites synthesized from coal fly ash.[21–23]

Fine grain materials, including nanomaterials, have been employed successfully in various fields, such as medical research, catalysis, and other fields, owing to their unique characteristics, including nanoscale size, large surface area, highly reactive porosity, hydrophilicity, and dispersibility.[1,24–26] In some literature, including our previous study, the characteristics of synthesized fine zeolite grains (or composites) and their capability to adsorb heavy metals have been partially assessed.[27–30] However, to the best of our knowledge, only a few literature studies have assessed the physicochemical characteristics of synthesized fine zeolite grains and their capability to adsorb heavy metals, including lead ions, from aqueous media.

Therefore, this study aims to explore the potential utilization of coal fly ash as a raw material to synthesize zeolites (adsorbent). Moreover, the capacity of the synthesized fine zeolite grains to adsorb lead ions and their adsorption mechanism are evaluated in detail.

## 2. Experimental section

### 2.1 Materials

Coal fly ash was obtained from the Tachibana-wan power station (Shikoku Electronic Power, Inc., Tokushima, Japan). Standard lead solution ($Pb(NO_3)_2$ in 0.1 mol $L^{-1}$ $HNO_3$) was purchased from FUJIFILM Wako Pure Chemical Co., Japan.

### 2.2 Preparation of zeolite grains and their characterization

The preparation method of fine zeolite grains and their physicochemical characteristics have been reported in our previous study.[27] A sodium-type zeolite was produced from coal fly ash *via* hydrothermal activation treatment.[18] Briefly, coal fly ash was mixed with sodium and heated. The obtained residue was used as the sodium-type zeolite (denoted as ZE) for removing lead ions. Moreover, dry milling treatment or wet dry milling treatment with ZE (each denoted as D-ZE and W-ZE, respectively) was applied for obtaining fine grains. Briefly, the dry milling treatment is as follows: ZE and zirconium beads of 0.5 mm diameter were mixed and crushed using a Shake Master NEO (Bio-Medical Science Cp., Ltd, Tokyo, Japan) at 1500 rpm for 3 h

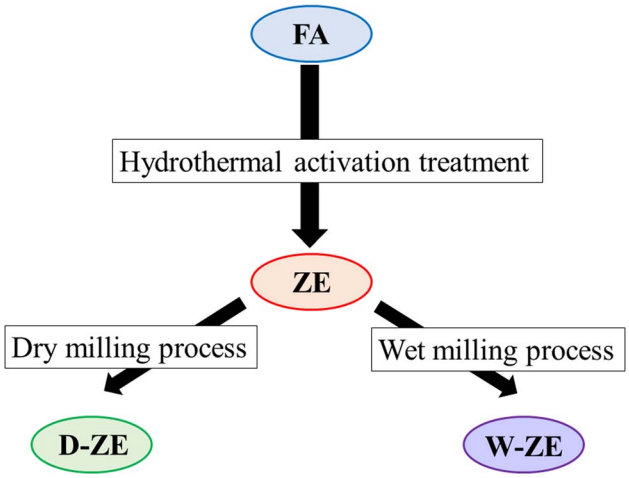


Fig. 1 Scheme of the preparation of ZE samples from coal fly ash.

(D-ZE). In addition, ZE was triturated using a pestle and mortar for 30 min. Then the triturated ZE was added to distilled water and milled using a Nano Pulverizer NP-100 (2000 rpm for 5 min × 3 times, 4 °C). The wet-milled sample was denoted as W-ZE (Fig. 1).

The physicochemical characteristics of ZE, D-ZE, and W-ZE were investigated including the morphology monitored using a scanning electron microscope (SEM) (Hitachi High-Technologies, Co., Tokyo, Japan), the X-ray diffraction (XRD) patterns were recorded using a MiniFlex II instrument (Rigaku, Osaka, Japan), the FTIR spectra were recorded using an FTIR-460Plus spectrometer (JASCO, Co., Japan), and the cation exchange capacity (CEC) was determined using the Japanese Industrial Standard method.[31] Additionally, a *NOVA4200e* (Yuasa Ionics, Japan) was used to determine the specific surface area and pore volume.

### 2.3 Adsorption capacity of lead ions

The capacity of lead ion adsorption was used as a screening criterion. Initially, 50 mL of 50 mg $L^{-1}$ lead-ion solution was mixed with 0.05 g of tested sample at 100 rpm for 24 h at 25 °C. Then, the filtrate obtained from a 0.45 μm membrane filter was collected. The equilibrium concentration of lead ions was measured using an iCAP-7600 Duo instrument (ICP-OES, Thermo Fisher Scientific Inc., Japan) and amount adsorbed was calculated by the differences between the initial and equilibrium concentrations.

Second, the effect of solution pH on the adsorption of lead ions was examined. For this, the pH of the sample solution was adjusted between 1, 3, 5, and 7 using a nitric acid or sodium hydroxide solution. Third, the effect of initial concentration on the adsorption capability was also examined by recording the adsorption isotherms using the aforementioned conditions. For this, the initial concentration was changed to 10, 20, 30, 40, and 50 mg $L^{-1}$ at 7 °C or 25 °C. The temperature was controlled at 25 °C with a water bath shaker MM-10 (TAITEC Co., Saitama, Japan). On the other hand, the 7 °C solution was prepared as follows: the sample solution was set at 5 °C in a water bath

 

shaker personal-11 (TAITEC Co., Saitama, Japan) in a low-temperature room at 6 °C. Finally, the effect of contact time on the adsorption capability was evaluated. The contact time was determined to be 0.5–24 h under our experimental conditions.

To elucidate the adsorption mechanism of lead ions from aqueous solutions using the prepared adsorbents, binding energy and elemental distribution before and after adsorption were assessed using ICP-OES, an AXIS-NOVA instrument (Shimadzu Co., Kyoto, Japan), and a JXA-8530F instrument (JEOL, Tokyo, Japan), respectively.

# 3. Results and discussion

## 3.1 Characteristics of the prepared adsorbents

As mentioned earlier, our previous study reported the physico-chemical characteristics of the prepared adsorbents.[27] Briefly, the mean particle sizes of the ZE, D-ZE, and W-ZE samples were 16.4 ± 0.4, 1.10 ± 0.3, and 0.55 ± 0.3 μm, respectively. These results indicate that the dry or wet milling process using ZE decreased the particle sizes and increased the specific surface areas. These changes positively influence the contact frequency between the prepared adsorbent and the target heavy metal (lead ions in this study). The FT-IR spectra results exhibited H–O–H bending, Si–O–Si (or Al–O–Si) asymmetric stretching, and Al–O–Al stretching vibration in ZE, D-ZE, and W-ZE, respectively. The structures of the ZE, D-ZE, and W-ZE absorbents comprised mullite, quarts, hydrosodalite, and zeolite P. However, in terms of crystallinity, the prepared adsorbents exhibited the following order: ZE > D-ZE > W-ZE. Moreover, the values of the CEC, specific surface area, and pore volume of the prepared adsorbents were in the order of ZE (42 mmol $g^{-1}$, 24 $m^2$ $g^{-1}$, and 1.3–62 μL $g^{-1}$) < D-ZE (72 mmol $g^{-1}$, 67 $m^2$ $g^{-1}$, and 7.2–180 μL $g^{-1}$) < W-ZE (135 mmol $g^{-1}$, 177 $m^2$ $g^{-1}$, and 12–327 μL $g^{-1}$). These findings indicate that novel adsorbents could be prepared using the combination of hydrothermal activation treatment and fine crystallization *via* the dry and/or wet milling process under our experimental conditions.

## 3.2 Quantity of lead ions adsorbed using the ZE samples under different pH conditions

The pH of the solution is one of the most critical variables and regulatory parameters in the adsorption procedures of heavy metals including lead ions from aqueous phases. The pH of the solution influences not only the adsorbent surface charge, but also the extent of ionization and sorbent speciation throughout the adsorption process.[32] Thus, the effect of pH on the adsorption of lead ions using the ZE samples is exhibited in Fig. 2. A previous study has found that when the potential precipitation of hydroxides and the type of speciation are controlled, the adsorption of heavy metals, including lead ions, is sensitive to pH variation.[33] At pH < 4.0, the adsorption capacity of lead ions on the ZE sample was small, while at pH 4–7, the adsorption capacity exhibited a steep increasing trend. At pH > 7, the adsorption capacity was maintained or slightly decreased in this study. At low pH, the lead ions were difficult to

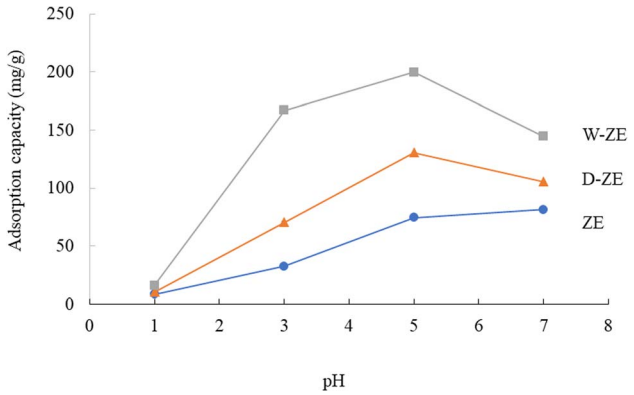


Fig. 2 Effect of pH on the adsorption of lead ions using ZE samples. Initial concentration: 50 mg $L^{-1}$, sample volume: 50 mL, adsorbent: 0.01 g, pH: 1, 3, 5, and 7, temperature: 25 °C, contact time: 24 h, and 100 rpm.

adsorb probably due to the competition between the excess protons ($H_3O^+$) and lead ions on the adsorbent surface. Thus, the increase in the pH value led to the augmentation of the adsorption capacity of lead ions. Moreover, $Pb(OH)_2$ precipitation occurred when the pH was ~6.5. The pH of the solution (initial pH was 5 and/or 7) increased to 6.5 or above after adsorption under our experimental conditions, indicating that these phenomena deregulated the effect of adsorption. Therefore, initial pH at 5 and/or 7 was not suitable for the removal of lead ions from the aqueous phase. Finally, the optimal pH value was 3 in this study. Furthermore, from several previous studies, the adsorption capacity of heavy metals increased with increasing pH values up to a neutral value and then decreased with increasing pH.[32] Similar trends were observed in this study. The consequence of pH could also be described in terms of the pH at the point of zero charge, at which the charge on the surface adsorbent is zero. Therefore, further studies are necessary for elucidating the adsorption efficiency of lead ions using ZE samples in the field.

## 3.3 Adsorption capacity of lead ions using the prepared ZE adsorbents

The adsorption capacity of lead ions using ZE samples was in the following order: ZE (32.7 mg $g^{-1}$) < D-ZE (70.7 mg $g^{-1}$) < W-ZE (166.9 mg $g^{-1}$). The correlation coefficient between the adsorption capacity and the CEC, specific surface area, micropore, mesopore, macropore, and total pore volume was 0.999, 1.000, 0.954, 0.983, 0.945, and 0.999, respectively (Fig. 3). These results indicated that the adsorption of lead ions was affected by these parameters of ZE samples.

## 3.4 Adsorption isotherms of lead ions using the ZE samples

The adsorption isotherms of ZE samples on lead ions are exhibited in Fig. 4. The results demonstrated that the number of adsorbed lead ions using the ZE samples increased with increasing temperatures (7 °C < 25 °C). These phenomena indicate that chemisorption is involved in the adsorption of lead ions. As mentioned above and/or below (Sections 3.2 and

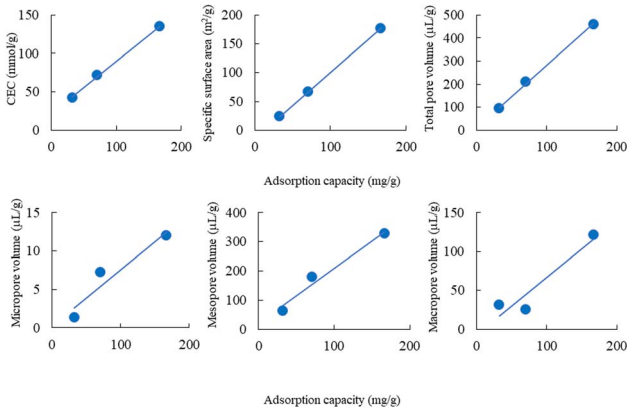


Fig. 3 Relationship between the number of lead ions and physicochemical characteristics.

3.5), the adsorption capacity of lead ions using ZE samples is related to the adsorbent surface and a chemical adsorption process involving valences through the exchange of electrons between the adsorbent and adsorbate. Moreover, the adsorption capacity of the tested adsorbents was in the order of ZE < D-ZE < W-ZE. This phenomenon can be due to the activation of adsorption sites on the ZE sample surface and increased lead reaction rate with these sites.[34] As mentioned in the above section, the surface characteristics and affinity of lead ions can be determined using the equilibrium adsorption isotherm constants that provide sufficient physicochemical data to identify the adsorption mechanism.[35] In this study, the Langmuir (eqn (1)) and Freundlich models (eqn (2)) were selected to evaluate the adsorption isotherms. The model equations are provided below.[36,37]

$$1/q = 1/(q_{max}K_L C_e) + 1/q_{max}, \quad (1)$$

$$\log q = \frac{1}{n}\log C_e + \log K_F, \quad (2)$$

where $q$ represents the adsorption capacity of lead ions (mg $g^{-1}$), $q_{max}$ represents the maximum adsorption capacity (mg $g^{-1}$), and $C_e$ represents the equilibrium concentration (mg $L^{-1}$). $K_F$ and $1/n$ represent the adsorption capacity and strength of adsorption, respectively. $K_L$ represents the Langmuir isotherm constant (binding energy) (L $mg^{-1}$).

The Langmuir model can theoretically explain monolayer adsorption onto a homogeneous surface, whereas the Freundlich model can empirically explain the monolayer adsorption onto a heterogeneous surface. Based on the correlation coefficient values of the Langmuir isotherm and Freundlich models, *i.e.*, 0.931–0.998 and 0.729–0.986, respectively, the obtained experimental data followed both the models (Table 1). Additionally, the maximum adsorption capacity ($q_{max}$) of lead ions increased with increasing adsorption temperature. These phenomena consist of the adsorption isotherm trends in Fig. 4. Finally, adsorption occurs when the value of $1/n$ lies between 01 and 0.5.[38] In this study, the value of $1/n$ (0.37–0.85) showed that the lead ions were easily adsorbed on the ZE samples.

Next, the elemental distribution of lead before and after adsorption is exerted in Fig. 5. As shown in the figure, the warm and cold colors indicate high and low concentrations of lead ions, respectively. The intensity of lead on the W-DE surface after adsorption increased compared to before adsorption. This finding indicates that lead ions were adsorbed on the surface of W-ZE. Furthermore, the peaks of lead ($4f_{5/2}$ and $4f_{7/2}$) were not detected before adsorption but were clearly found upon adsorption under our experimental conditions as shown in Fig. 6. These results suggest here that the physicochemical properties of the ZE sample surface greatly affect the adsorption capability of lead ions from aqueous media.

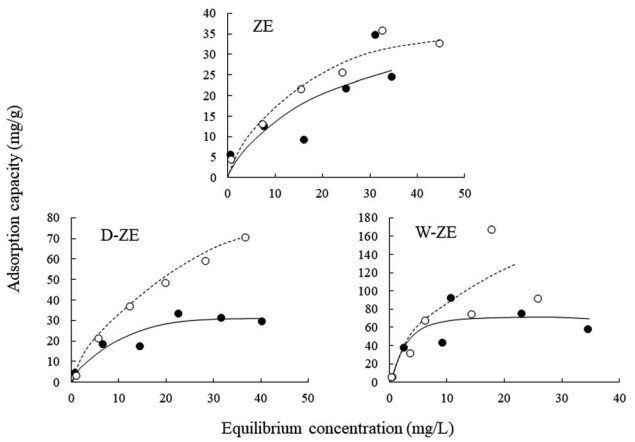


Fig. 4 Adsorption isotherms of lead ions using ZE samples. Initial concentration: 1, 10, 20, 30, 40, and 50 mg $L^{-1}$, sample volume: 50 mL, adsorbent: 0.01 g, temperature: 7 (●) and 25 (○) °C, contact time: 24 h, and 100 rpm.

Table 1 Langmuir and Freundlich constants for the adsorption of lead ions

| | | Langmuir isotherm model | | | Freundlich isotherm model | | |
|---|---|---|---|---|---|---|---|
| Adsorbents | Temperature (°C) | $K_L$ (L $mg^{-1}$) | $q_{max}$ (mg $g^{-1}$) | $r^2$ | $K_F$ | $1/n$ | $r^2$ |
| ZE | 7 | 0.57 | 22.8 | 0.931 | 6.18 | 0.37 | 0.729 |
| | 25 | 0.05 | 51.8 | 0.982 | 4.99 | 0.52 | 0.986 |
| D-ZE | 7 | 0.22 | 31.4 | 0.988 | 5.67 | 0.50 | 0.933 |
| | 25 | 0.04 | 107.5 | 0.998 | 3.73 | 0.85 | 0.976 |
| W-ZE | 7 | 0.07 | 138.9 | 0.978 | 12.7 | 0.58 | 0.764 |
| | 25 | 0.10 | 149.3 | 0.998 | 12.3 | 0.75 | 0.920 |

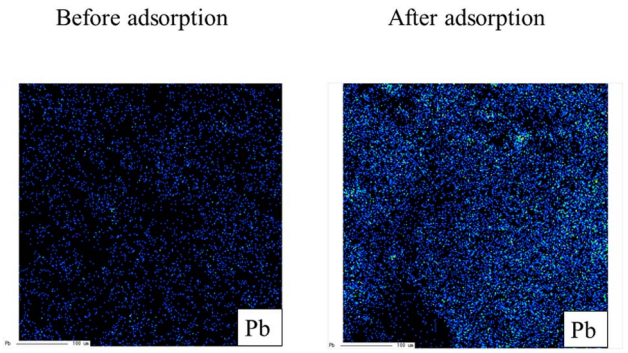


Fig. 5 Elemental distribution of lead (Pb) before and after adsorption. Initial concentration: 50 mg $L^{-1}$, sample volume: 50 mL, adsorbent: 0.01 g, temperature: 25 °C, contact time: 24 h, and 100 rpm.

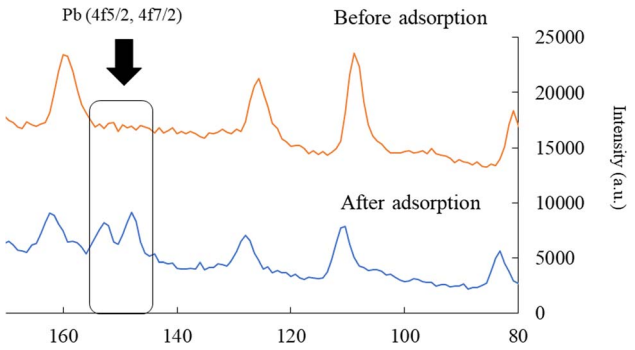


Fig. 6 Binding energy of lead (Pb) before and after adsorption. Initial concentration: 50 mg $L^{-1}$, sample volume: 50 mL, adsorbent: 0.01 g, temperature: 25 °C, contact time: 24 h, and 100 rpm.

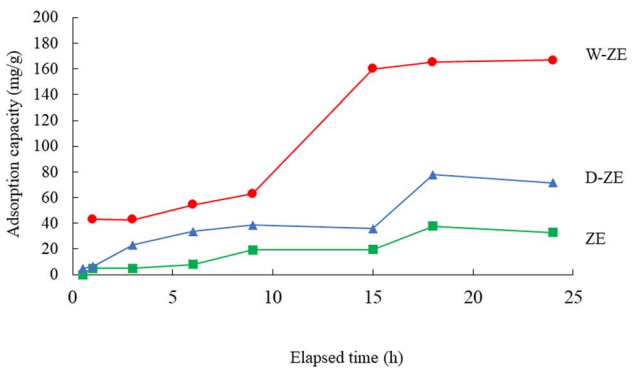


Fig. 7 Effect of contact time on the adsorption of lead ions using ZE samples. Initial concentration: 50 mg $L^{-1}$, sample volume: 50 mL, adsorbent: 0.01 g, pH: 3, temperature: 25 °C, contact time: 0.5, 1, 3, 6, 9, 15, 18, and 24 h, and 100 rpm.

### 3.5 Effect of contact time on the adsorption of lead ions using the ZE samples

Fig. 7 shows the effect of contact time on the adsorption of lead ions using the ZE samples. Adsorption capacity increased with elapsed time, and equilibrium adsorption was achieved at ~15 to 18 h. In particular, the amount adsorbed using W-ZE drastically increased between 10 and 15 h under our experimental conditions. In the initial stage, there were enough adsorption sites on the ZE samples surface, and the lead ion concentrations was high. The interaction between lead ions and the ZE sample surface easily occurred and led to gradual and/or drastic increase in the adsorption rate in the early and middle stages. On the other hand, as the number of adsorption sites decreases, the adsorption capacity onto ZE samples becomes close to saturation. Finally, the adsorption curve is basically a horizonal line under our experimental conditions.[39]

Adsorption kinetics provide information regarding adsorbate diffusion processes, adsorption rates, and rate-limiting steps.[40,41]

In this study, pseudo-first-order (eqn (3)) and pseudo-second-order (eqn (4)) models were selected for representing the kinetics of lead-ion adsorption from the aqueous media. These models can be expressed as follows:[42,43]

$$\ln(q_e - q_t) = \ln q_e - k_1 t, \quad (3)$$

$$\frac{t}{q_t} = \frac{t}{q_e} + \frac{1}{k_2 \times {q_e}^2}, \quad (4)$$

where $q_e$ (mg $g^{-1}$) represents the adsorption capacity of lead ions at equilibrium, $q_t$ (mg $g^{-1}$) represents the adsorption capacity of lead ions at time $t$, $k_1$ ($1/h$) represents the overall constant in the pseudo-first-order model, and $k_2$ (g $mg^{-1}$ $h^{-1}$) represents the pseudo-second-order adsorption constant.

The fitting results of kinetic data using the pseudo-first-order and pseudo-second-order models are shown in Table 2. As shown in the table, the best fitting of experimental data was observed in the pseudo-second-order model (correlation coefficient: 0.946–0.994) compared to the pseudo-first-order model (correlation coefficient: 0.918–0.960). The maximum adsorption capacity ($q_{e,cal}$) in the pseudo-second-order model increased in the order of ZE < D-ZE < W-ZE. These findings are in agreement with the results shown in Fig. 7 (adsorption kinetics data). Previous studies[43,44] have reported that a good fitting of data obtained from the pseudo-second-order model indicated that the adsorption process was based on chemisorption, which was related to the exchange or sharing of electrons between ZE samples and lead ions.

Table 2 Fitting results of kinetic data using PFOM and PSOM in a single solution system

| | | Pseudo-first-order model | | | Pseudo-second-order model | | |
|---|---|---|---|---|---|---|---|
| Adsorbents | $q_{e,exp}$ (mg $g^{-1}$) | $K_1$ (1/h) | $q_{e,cal}$ (mg $g^{-1}$) | $r$ | $K_2$ (mg $g^{-1}$ $h^{-1}$) | $q_{e,cal}$ (mg $g^{-1}$) | $r$ |
| ZE | 37.7 | 0.08 | 41.2 | 0.960 | 0.007 | 39.2 | 0.994 |
| D-ZE | 77.8 | 0.09 | 82.0 | 0.918 | 0.003 | 60.2 | 0.965 |
| W-ZE | 167.0 | 0.30 | 373.3 | 0.951 | 0.004 | 188.7 | 0.946 |

Table 3 Comparison of the lead ions adsorption capacity with those of other reported adsorbents

| Samples | Adsorption capability (mg $g^{-1}$) | pH | Temperature (°C) | Initial concentration (mg $L^{-1}$) | Contact time (h) | Adsorbent (g $L^{-1}$) | Ref. |
|---|---|---|---|---|---|---|---|
| Modified coal fly ash | 31.4 | 3 | 27 ± 2 | 1000 | 4 | 20 | Astuti *et al.* (2021) |
| Na–Y zeolite derived from coal gangue | 457 | 6 | 45 | 200 | 0.67 | 0.4 | Ge *et al.* (2020) |
| Zeolite synthesized from PCFA | 99.5 | 5 | 25 | 50 | 48 | 0.2 | Kobayashi *et al.* (2020) |
| Zeolite material synthesized from CFBFA | 424.7 | 6 | 25 | 500 | 1 | 0.2 | Ma *et al.* (2022) |
| Zeolite | 45.5 | — | 30 | 18 | 20 | 0.8 | Khan *et al.* (2021) |
| ZE | 32.7 | 3.0 | 25 | 50 | 24 | 0.2 | This study |
| D-ZE | 70.7 | 3.0 | 25 | 50 | 24 | 0.2 | This study |
| W-ZE | 166.9 | 3.0 | 25 | 50 | 24 | 0.2 | This study |

Finally, previous studies that removed lead ions from aqueous media using different types of adsorbents were compared with our study (Table 3).[45–49] The comparison shows that W-ZE is useful for removing lead ions from aqueous media (except for zeolite materials synthesized from circulating fluidized bed fly ash and coal gangue).

## 4. Conclusions

ZE, D-ZE, and W-ZE, were prepared, and its high adsorption capacity of lead ions by focusing the adsorption process with ZE, D-ZE, and W-ZE. The current results demonstrate that the adsorption capability of lead ions and the physicochemical characteristics of ZE samples, including their SEM images, XRD patterns, FTIR spectra, CEC, specific surface area, and pore volume, were in the following order: ZE < D-ZE < W-ZE. Additionally, the optimal adsorption conditions for using the ZE samples were as follows: (1) high adsorption temperatures (7 °C < 25 °C), (2) an acidic pH of 5.0, and (3) an equilibrium adsorption time of ~15 h. The obtained results fitted to a pseudo-second-order kinetic model and isotherm models, including the Langmuir and Freundlich models. Moreover, to elucidate the adsorption mechanism of lead ions using W-ZE, the elemental distribution and binding energy of the samples were analyzed before and after adsorption. It was observed that lead ions were present on the W-ZE surface. These results indicate that the physicochemical characteristics of the ZE samples strongly affect the adsorption capacity of lead ions from aqueous media. Finally, W-ZE appears to be a promising candidate for the adsorption of lead ions from aqueous media.

## Author contributions

Fumihiko Ogata: conceptualization, project administration, writing – original draft, and writing–review & editing; Noriaki Nagai: investigation, methodology, and visualization; Yugo Uematsu: investigation and visualization; Yuhei Kobayashi: investigation and visualization; Nanako Kitamura: investigation and visualization; Chalermpong Saenjum: investigation and visualization; Naohito Kawasaki: project administration, supervision, and writing – review & editing.

## Conflicts of interest

There are no conflicts to declare.

## Acknowledgements

This work is supported by JSPS KAKENHI (JP22K06674).

## References

1 K. Shamshad, N. Mu, A. G. Adel and I. Jibran, Engineering nanoparticles for removal of pollutants from wastewater: current status and future prospects of nanotechnology for remediation strategies, *J. Environ. Chem. Eng.*, 2021, **9**, 106160.
2 O. A. Uyiosa, E. U. Kingsley, B. O. Robert, A. O. Otolorin, D. Handoko and S. K. Heri, Fly ash-based adsorbent for adsorption of heavy metals and dyes from aqueous solution: a review, *J. Mat. Res. Technol.*, 2021, **14**, 2751–2774.
3 WHO, *Guideline for Drinking-Water Quality*, WHO Library Cataloguing-in-Publication Data, Geneva, vol. 1, 2006.
4 *ATSDR's Substance Priority List, the Agency for Toxic Substances and Disease Registry*, ATSDR, 2017.
5 *International Agency for Research on Cancer Monographs on the Identification of Carcinogenic Hazardous to Humans, List of Classifications*, WHO, 2006.
6 A. Khalil, S. Habib-ur-Rehman, S. K. Muhammad, I. Amjad, P. Erich, S. A. Larissa, R. Sidra, N. Haq, A. Asif, N. Khalida, M. Ali, R. Y. Muhammad and A. Muhammad, Lead in drinking water: adsorption method and role of zeolite imidazolate frameworks for its remediation: a review, *J. Clean. Prod.*, 2022, **368**, 133010.
7 Z. Shariatinia and A. Bagherpour, Synthesis of zeolite NaY and its nanocomposites with chitosan as adsorbents for lead(II) removal from aqueous solution, *Powder Technol.*, 2018, **338**, 744–763.

8 A. M. Safruk, E. McGregor, M. L. W. Asulund, P. H. Chueng, C. Pinsent, B. J. Jackson, A. T. Hair, M. Lee and E. A. Sigal, The influence of lead content in drinking water, household dust, soil, and paint on blood lead levels of children in Flin Flon, Manitoba and Creighton, Saskatchewan, *Sci. Total Environ.*, 2017, **593–594**, 202–210.

9 Y. Zhou, X. Liu, L. Tang, F. Zhang, G. Zeng, X. Peng, L. Lou, Y. Deng, Y. Pang and J. Zhang, Insight into highly efficient co-removal of p-nitrophenol and lead by nitrogen-functionalized magnetic ordered mesoporous carbon: performance and modelling, *J. Hazard. Mat.*, 2017, **333**, 80–87.

10 E. I. Unuabonah, K. O. Adebowale, B. I. Olu-Owolabi, L. Z. L. Yang and X. Kong, Adsorption of Pb(II) and Cd(II) from aqueous solutions onto sodium tetraborate-modified Kaoline clay: equilibrium and thermodynamic studies, *Hydrometallurgy*, 2008, **93**, 1–9.

11 I. S. Bădescu, D. Bulgariu, I. Ahmad and L. Bulgariu, Valorisation possibilities of exhausted biosorbents loaded with metal ions-a review, *J. Environ. Manage.*, 2018, **224**, 288–297.

12 Z. T. Yao, X. S. Ji, P. K. Sarker, J. H. Tang, L. Q. Ge, M. S. Xia and Y. Q. Xi, A comprehensive review on the applications of coal fly ash, *Earth Sci. Rev.*, 2015, **141**, 105–121.

13 J. R. Pan, C. Huang, J. Kuo and S. H. Lin, Recycling MSWI bottom and fly ash as raw materials for Portland cement, *Waste Manage.*, 2008, **28**, 1113–1118.

14 F. Zhu, M. Takaoka, K. Oshita and S. Morisawa, The calcination process in a system washing, calcinating, and converting treated municipal waste incinerator fly as into raw material for the cement industry, *J. Air Waste Manage. Assoc.*, 2011, **61**, 740–746.

15 W. Franus, M. Wdowin and M. Franus, Synthesis and characterization of zeolites prepared from industrial fly ash, *Environ. Monit. Assess.*, 2014, **186**, 5721–5729.

16 R. S. Blissett and N. A. Rowson, A review of the multi-component utilization of coal fly ash, *Fuel*, 2012, **97**, 1–23.

17 C. G. Flores, H. Schneider, N. R. Marcillio, L. Ferret and J. C. P. Oliveira, Potassic zeolites from Brazilian coal ash for use as a fertilizer in agriculture, *Waste Manage.*, 2017, **70**, 263–271.

18 Y. Kobayashi, F. Ogata, T. Nakamura and N. Kawasaki, Synthesis of novel zeolites produced from fly ash by hydrothermal treatment in alkaline solution and its evaluation as an adsorbent for heavy metal, *J. Environ. Chem. Eng.*, 2020, **8**, 103687.

19 Z. M. Ayalew, X. Zhang, X. Guo, S. Ullah, S. Leng, X. Luo and N. Ma, Removal of Cu, Ni and Zn directly from acidic electroplating wastewater by oligo-ethyleneamine dithiocarbamate (OEDTC), *Sep. Purif. Technol.*, 2020, **248**, 117114.

20 W. Astushi, R. A. Hermawan, H. Mukti and N. R. Sugiyono, Preparation of activated carbon from mangrove propagule waste by $H_3PO_4$ activation for $Pb^{2+}$ adsorption, *AIP Conf. Proc.*, 2017, **1788**, 030082.

21 A. Hamadi and K. Nabih, Alkali activation of oil shale ash based ceramics, *Chem.–Eur. J.*, 2012, **9**(3), 1373–1388.

22 H. Bergk, M. Porsch and J. Drews, Conversion of solid primary and recycled raw materials to zeolite-containing products. Part VI: continuous manufacture of zeolite A containing products, *Chem. Technol.*, 1987, **39**, 308–310.

23 F. Mondragon, F. Rincon, L. Sierra, J. Escobar, J. Ramırez and J. Fernandez, New perspectives for coal ash utilization: synthesis of zeolitic materials, *Fuel*, 1990, **69**(2), 263–266.

24 S. Khan, R. Anjum and M. Bilal, Revealing chemical speciation behaviors in aqueous solutions for uranium(VI) and europium(III) adsorption on zeolite, *Environ. Technol. Innovation*, 2021, **22**, 101503.

25 Y. Wu, H. Pang, Y. Liu, X. Wang, S. Yu, D. Fu, J. Chen and X. Wang, Environmental remediation of heavy metal ions by novel-nanomaterials: a review, *Environ. Pollut.*, 2019, **246**, 608–620.

26 S. Khan, H. Sengül and Z. Dan, Transport of $TiO_2$ nanoparticles and their effects on the mobility of Cu in soil media, *Desalin. Water Treat.*, 2018, **131**, 230–237.

27 F. Ogata, N. Nagai, C. Ito, Y. Kobayashi, M. Yamaguchi, A. Tabuchi, C. Saenjum, T. Nakamura and N. Kawasaki, Improvement in adsorption of $Hg^{2+}$ from aqueous media using sodium-type fine zeolite grains, *Water Sci. Technol.*, 2022, **85**, 2827.

28 Z. Shariatinia and A. Bagherpour, Synthesi of zeolite NaY and its nanocomposites with chitosan as adsorbents for lead(II) removal from aqueous solution, *Powd. Technol.*, **338**, 744–763.

29 M. Irandoost, M. Pezeshki-Modaress and V. Javanbakht, Removal of lead from aqueous solution with nanofibrous nanocomposite of polycaprolactone adsorbent modified by nanoclay and nanozeolite, *J. Water Proc. Eng.*, 2019, **32**, 100981.

30 E. A. Abdelrahma, A. Alharbi, A. Subaihi, A. M. Hameed, M. A. Almutairi, F. K. Algethami and H. M. Youssef, Facile fabrication of novel analcime/sodium aluminum silicate hydrate and zeolite Y/faujasaite mesoporous nanocomposites for efficient removal of Cu(II) and Pb(II) ions from aqueous media, *J. Mat. Res. Technol.*, 2020, **9**, 7900–7914.

31 *Test Method of Cation Exchange Capacity for Artificial Zeolite, JIS K 1478*, 2009.

32 U. O. Aigbe, K. E. Ukhurebor, R. B. Onyancha, O. A. Osibote, H. Darmokoesoemo and H. S. Kusuma, Fly ash-based adsorbent for adsorption of heavy metals and dyes from aqueous solution: a review, *J. Mater. Res. Technol.*, 2021, **14**, 2751–2774.

33 G. Bayramoglu and M. Y. Arica, Adsorption of Cr(VI) onto PEI immobilized acrylate-based magnetic beads: isotherms, kinetics and thermodynamic study, *Chem. Eng. J.*, 2008, **139**(1), 20–28.

34 Z. Shariatinia and A. Bagherpour, Synthesis of zeolite NaY and its nanocomposites with chitosan as adsorbents for lead(II) removal from aqueous solution, *Powder Technol.*, 2018, **338**, 744–763.

35 I. Langmuir, The adsorption of gases on plane surfaces of glass, mica and platinum, *J. Am. Chem. Soc.*, 1918, **40**, 1361–1403.

36 H. Freundlich, Over the adsorption in solution, *J. Phys. Chem.*, 1906, **57**, 384–471.
37 I. Abe, M. Hayashi and M. Kitagawa, Studies on the adsorption of surfactants on activated carbon, *J. Jpn. Oil Chem. Soc.*, 1976, **25**, 145–150.
38 R. Peña Penilla, A. Guerrero Bustos and S. Goñi Elizalde, Immobilization of Cs, Cd, Pb and Cr by synthetic zeolites from Spanish low-calcium coal fly ash, *Fuel*, 2006, **85**, 823–832.
39 Z. Wnag, W. Xu, F. Jie, Z. Zhang, K. Zhou and H. Liu, The selective adsorption performance and mechanism of multiwall magnetic carbon nanotubes for heavy metals un wastewater, *Sci. Rep.*, 2021, **11**, 16878.
40 Y. Liu, C. Yan, Z. Zhang, H. Wang, S. Zhou and W. Zhou, A comparative study on fly ash, geopolymer and faujasite block for Pb removal from aqueous solution, *Fuel*, 2016, **185**, 181–189.
41 M. Uğurlu and M. Hamdi Karaoğlu, Adsorption of ammonium from an aqueous solution by fly ash and sepiolite: isotherm, kinetic and thermodynamic analysis, *Microporous Mesoporous Mater.*, 2011, **139**, 173–178.
42 D. Karamanis and P. A. Assimakopoulos, Efficiency of aluminum-pillared montmorillonite on the removal cesium and copper from aqueous solution, *Water Res.*, 2007, **41**, 1897–1900.
43 Y. S. Ho and G. MacKay, Pseudo-second-order model for sorption process, *Process Biochem.*, 1999, **34**, 451–465.
44 M. Jovanovic, N. Rajic and B. Obradovic, Novel kinetic model of the removal of divalent heavy metal ions from aqueous solutions by natural clinoptilolite, *J. Hazard. Mater.*, 2012, **233–234**, 57–64.
45 W. Astuti, A. Chafidz, A. S. Al-Fatesh and A. H. Fakeeha, Removal of lead(PB(II)) and zinc (Zn(II)) from aqueous solution using coal fly ash (CFA) as a dual-sites adsorbent, *Chin. J. Chem. Eng.*, 2021, **34**, 289–298.
46 Q. L. Ge, M. Moeen, Q. Tian, J. J. Xu and K. Q. Feng, Highly effective removal of $Pb^{2+}$ in aqueous solution by Na-X zeolite derived from coal gangue, *Environ. Sci. Pollut. Res.*, 2020, **27**(7), 7398–7408.
47 Y. Kobayashi, F. Ogata, C. Saenjum, T. Nakamura and N. Kawasaki, Removal of $Pb^{2+}$ from aqueous solutions using K-type zeolite synthesized from coal fly ash, *Water*, 2020, **12**(9), 2375–2386.
48 Z. Ma, X. Zhang, G. Lu, Y. Guo, H. Song and F. Cheng, Hydrothermal synthesis of zeolitic material from circulating fluidized bed combustion fly ash for the highly efficient removal of lead from aqueous solution, *Chin. J. Chem. Eng.*, 2022, **47**, 193–205.
49 S. Khan, M. Idrees and M. Bilal, Revealing and elucidating chemical speciation mechanisms for lead and nickel adsorption on zeolite in aqueous solutions, *Colloids Surf., A*, 2021, **623**, 126711.